Tumbling is general

This project is maintained by Julia Lazzari-Dean in the York lab, and was funded by Calico Life Sciences LLC

Research article

From cameras to confocal to cytometry: measuring tumbling rates is a general way to reveal protein binding

Julia R. Lazzari-Dean (ORCID)[1*], Austin E.Y.T. Lefebvre[1], Rebecca Frank Hayward[1], Lachlan Whitehead[2,3], Maria Ingaramo[1†], Andrew G. York[1‡]

[1]*Calico Life Sciences LLC, South San Francisco, CA 94080, USA*

[2]*Walter and Eliza Hall Institute of Medical Research, Parkville, Victoria, Australia*

[3]*Department of Medical Biology, University of Melbourne, Parkville, Victoria, Australia*

[*]*Permanent email: julia.lazzaridean+tumbling@gmail.com*

[†]*Permanent email: maria.del.mar.ingaramo+tumbling@gmail.com*

[‡]*Permanent email: andrew.g.york+tumbling@gmail.com*

Pre-print published: TODO

Please cite as: TODO

Abstract

Molecular interactions are central to understanding any biological system, but they are labor-intensive to measure with existing optical approaches. Tracking "tumbling" (rotational diffusion) is a generalizable strategy for determining particle size, from which the presence and size of binding partners in a complex can be inferred. However, fluorescence-based tumbling measurements have historically been limited to small targets (<30 kDa) due to the short (nanosecond) lifetime of typical fluorophores. This

size limit leaves most of the proteome inaccessible, severely limiting the usefulness of the approach. To reveal larger complexes and realize the full potential of optical tumbling measurements, several groups have explored longer-lived states, such as photobleached molecules**,** reversibly photoswitched proteins**, or** triggerable triplets**. Here, we describe four combinations of photophysics and hardware for measuring tumbling with longer-lived states, gearing each toward a candidate biological use case. We explore these four measurement schemes with simulations and, in one case, experimentally validate the approach. Our work suggests that, with minor reconfiguring, most fluorescence approaches to detect the presence of proteins could also reveal their binding state.**

Figure 1: Introduction to optical measurements of protein binding with tumbling.

1. 0:03 Particle size affects the rate of tumbling, with larger particles tumbling more slowly than smaller ones. Binding of another protein increases a protein's effective size.
2. 0:20 The probability of absorption of polarized light depends on fluorophore orientation. Fluorophores with dipoles aligned with the light's polarization are more likely to absorb it.
3. 0:42 A pulse of polarized light selects a partially aligned subpopulation of fluorophores. This subpopulation scrambles its alignment over time as it tumbles.
4. 1:07 Each chemical species has its own characteristic tumbling rate; binding or dissociation will change the relative abundance of these tumbling rates.

Cartoon structures are from the RCSB PDB (4EUL, 6NYB). Please note that rotation and translation in this conceptual animation are ballistic, which does not accurately represent the diffusive motion of proteins in solution.

We find that, while inaccurate, this improves communication. Please refer to Figure 2 for more physically representative diffusive motion.

Note that this is a limited PDF or print version; animated and interactive figures are disabled. For the full version of this article, please visit https://andrewgyork.github.io/tumbling_is_general

Introduction

For 4 billion years, molecular interactions have been essential for life. Each protein, nucleic acid, or lipid in a cell is a character in a chaotic play, zooming from place to place and dancing with different partners to ultimately produce the complex behaviors of living creatures. Mapping out this cascade of interactions is a recurring challenge across the biological sciences.

Fluorescence microscopy reveals where molecules are, and with some care, it can also report their abundance [Lakowicz 2006]. Location is a clue about function, but it's only part of the picture. To better understand function, we'd like to monitor the interactions (binding) of our protein of interest in real time in its native context. Unfortunately, fluorescence microscopy is blind to binding information without complicated add-ons, each with considerable downsides (e.g. FRET, FCS, or SPT, discussed in the Appendix).

How might we extract binding information from a generalizable optical readout? Binding changes a molecule's effective size, and different binding partners yield complexes of different sizes. Conveniently, the size of a protein complex is inversely proportional to its rate of “tumbling” (rotational diffusion), with larger complexes tumbling more slowly than smaller complexes (Figure 1 0:03, Figure 2). Therefore, if we can measure tumbling rate, we can reveal molecular interactions.

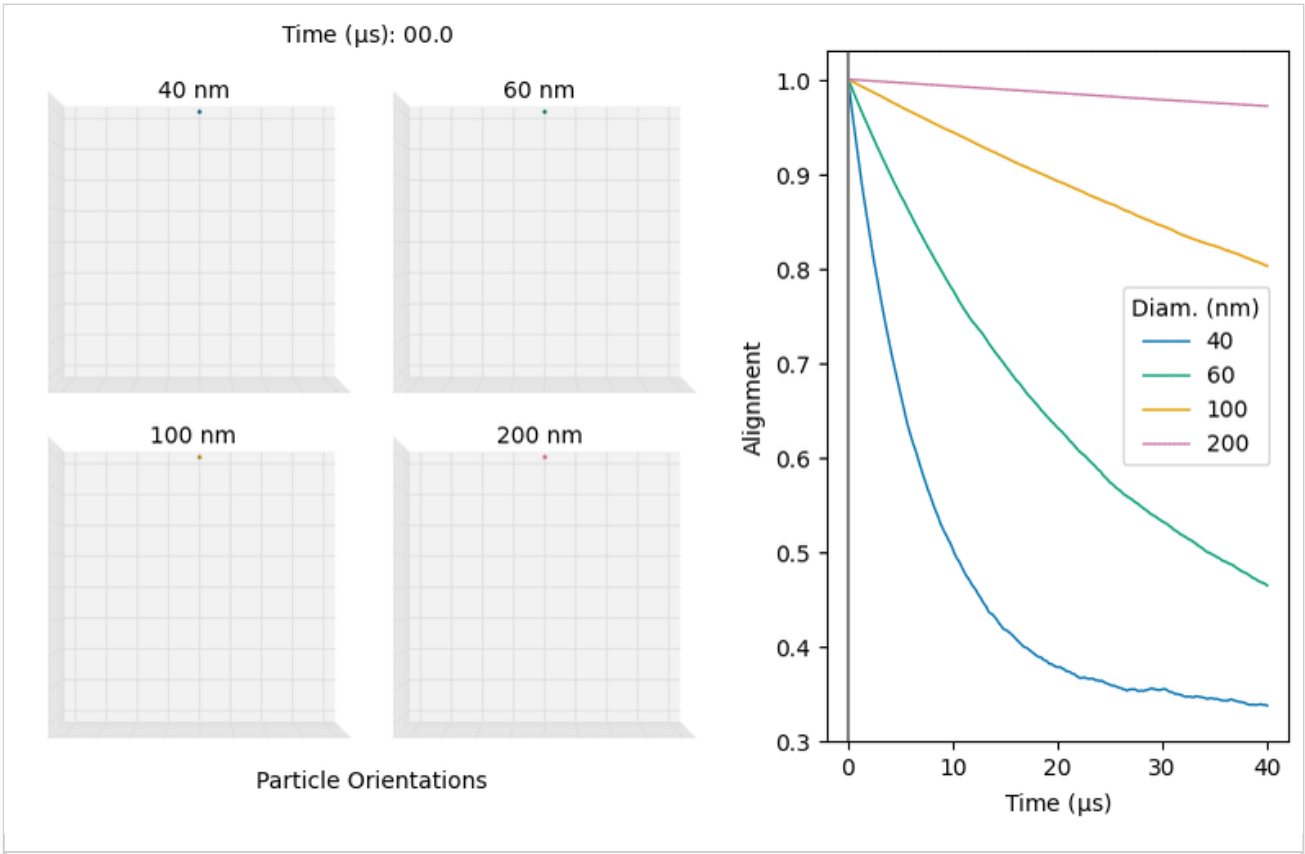

Initial Distribution: North Pole

Figure 2: Scrambling rate of initially-aligned particles depends on their size.
Simulation of 40, 60, 100, and 200 nm diameter particles (tumbling times 22, 73, 340, and 2718 µs respectively) decaying from an initial orientation distribution. Points on the sphere represent molecular orientations (analogous to the arrow bouquet diagrams in Figure 1 0:42). The alignment of the population decreases over time as the particles tumble. This simulation models realistic diffusive rotation, building on the conceptual rendition in Figure 1. Drop-down options toggle the initial distributions: (1) "north pole", or an artificial initial distribution of axially aligned molecules, (2) a “cap” distribution generated by non-saturating photoselection with linearly polarized light, and (3) a “crescent” pattern as would be generated by (2) followed by a saturating orthogonally polarized depletion beam [York 2019].

The most common optical strategy for measuring tumbling is fluorescence anisotropy [Weber 1952], which reports how much and how fast the alignment of a population of fluorophores scrambles during its fluorescence lifetime. Excitation with polarized light selects an initial, partially aligned subpopulation. The more aligned a ground state fluorophore's absorption dipole is with the incoming light polarization, the more likely it is to absorb that light (Figure 1 0:20). Following absorption, fluorescence emission typically occurs over a few nanoseconds (the fluorescence lifetime), during which tumbling scrambles alignment (Figure 1 0:42). The more aligned the fluorophores' dipoles are when emission occurs, the more polarized the emission is. Slower rotating populations stay more aligned over time and therefore emit more polarized fluorescence (Figure 1 1:07).

For small targets that tumble detectably during the fluorescence lifetime, fluorescence anisotropy allows *in situ* monitoring of binding. Larger (>30 kDa) targets emit light before appreciable scrambling occurs and thus all appear the same; for example, fluorescence anisotropy cannot distinguish a 100 kDa from a 200 kDa target. Unfortunately, existing live cell fluorophore tags (e.g. GFP, HaloTag [Los 2008], SNAP-tag [Juillerat 2003]) are 20-30 kDa, using up much of the accessible size range. Even if a massless tag were developed, the median size of a eukaryotic protein is 50 kDa [Netzer 1998], so *almost all protein complexes tumble too slowly to be interrogated with fluorescence anisotropy.*

With tumbling, the accessible size range is proportional to the observation time window. If we extend the time window to microseconds or beyond, we can reveal many protein-protein interactions. Recognizing the value of this approach, experimenters have tried to use various long-lived states for tumbling. For example, phosphorescence emission can reveal tumbling on the millisecond time scale [Austin 1979, Moore 1979]. Alternatively, polarized photobleaching produces an infinitely-long-lived bleached state; the remaining unbleached ground state molecules can reveal tumbling occurring in a few microseconds or up to seconds [Smith 1981, Velez 1988]. Despite having been around for decades, these techniques are not widely used to measure protein-protein interactions. Phosphorescence is limited by very low signal in the relevant time window. The damage caused to samples by photobleaching is unappealing for time course imaging, but given the simplicity of the approach, we aren't sure why it isn't more widely used.

The discovery of long-lived states with triggerable emission in fluorescent proteins has opened up exciting new possibilities for tumbling measurements on protein complexes. [Volpato 2023]

used the active state of a reversible switchable fluorescent protein (rsFP) to monitor tumbling over long timescales. Building on this work, [Lu 2023] showed the same principle applies with triggerable fluorescence from a triplet state (termed "optically activated delayed fluorescence"). Beyond just extending the size range, these "triggerable emitters" offer a crucial level of control over the timing of photon production. Unlike fluorescence or phosphorescence, where photons are emitted spontaneously over a defined lifetime, triggerable emitters produce photons on demand, allowing the experimenter to concentrate their limited photon budget into times when it is maximally informative. The value of certain measurement times over others can be seen in Figure 2, where the alignment difference between the 100 and 200 nm beads is much larger at 20 μs than at 2 μs. Thus, triggerable emitters improve both the size range and the signal-to-noise ratio of a tumbling measurement.

The triggerable emitters explored by [Volpato 2023] and [Lu 2023] enable new pulse schemes and hardware configurations ranging far beyond the point-scanning confocal approach typically used for fluorescence anisotropy; this space is largely unexplored. In this work, we explore tumbling with three different photophysics (photobleaching, rsFPs, triggered triplets) and four hardware configurations (a cheap handheld device, a high data rate microscope, a flow cytometer, and a commercially available microscope). To facilitate these investigations, we develop and apply open-source simulation code. We simulate four case studies, each optimized towards a different application, and we obtain experimental data on the commercial instrument. In the future, we envision that tumbling measurements will be possible on most imaging hardware, as available as red and green color channels are today.

Results and Discussion

Tumbling Simulation Code

In gas phase, the mean collision time is much longer than the rotation time, so molecules (e.g. N_2 at room temperature and ambient pressure) execute many rotations before the speed and direction of rotation is disrupted by their neighbors [Felker 1986]. This "ballistic" motion is what we illustrate in Figure 1, which is aesthetically pleasant but inaccurate for proteins in solution. In liquids, the mean collision time is effectively zero, so we simulate the orientation versus time of each molecule in our ensemble as a random walk on the surface of a sphere, with an angular step size $d\theta = \sqrt{\frac{2t}{\tau}}$, where t is time and τ is the tumbling time [Ghosh 2013]. This correct, diffusive motion is simulated and displayed in Figures 2-6.

Our code simulates the stochastic dynamics of the orientation and photophysical state of each molecule in an ensemble. We model two types of state transitions: spontaneous and light-driven. Spontaneous transitions occur with constant probability per unit time, and the transition times are therefore drawn from an exponential distribution parameterized by its lifetime. For example, a fluorescent excited state decays to the ground state with a lifetime of a few nanoseconds. Light-driven transitions are instantaneous in our simulations, and their probability depends on molecular alignment with respect to the illumination polarization. For example, a ground state molecule absorbs light and enters the excited state. For light-driven transitions, we choose to specify light intensity in "saturation units," where intensity x excites a fraction of perfectly aligned molecules equal to $1 - 2^{-x}$. The effective intensity that a fluorophore sees is proportional to $\cos^2(\theta)$, where θ is the angle between its orientation (absorption dipole) and the polarization of the incoming light. We simulate the case where the fluorophores' absorption and emission dipoles are parallel. This assumption is approximately correct for fluorescence excitation and emission [Lakowicz 2006, Myšková 2020], incorrect for rsFP activation and excitation [Yadav 2015], and likely incorrect for triplet triggering and emission [Lettinga 2000]. In the cases we simulate, we believe that angular disagreement between the dipoles reduces the mass resolution without changing the mass range.

In a typical tumbling simulation or measurement, polarized light illuminates a population of fluorophores, and their emission is split between two detectors by a polarizing beamsplitter. One detector collects light with polarization parallel (∥) to an external reference (e.g. an input beam polarized in the Y direction); the other detector collects light with polarization perpendicular (⊥) to that reference (e.g. the X direction). We sometimes represent the relative amounts of these two signals as the polarization, which ranges from 1 (all ∥) to -1 (all ⊥). Immobile, randomly oriented fluorophores excited with linearly polarized light fluoresce with a polarization of 0.5 (3:1 ∥:⊥ ratio) [Lakowicz 2006]. If fluorophores scramble their alignment completely before they emit, the polarization of their fluorescence will be 0. Tumbling times that are similar to the observation time window result in polarization between 0 and 0.5.

We suspect that much of the benefit of the simulation code lies in empowering others to use it. In that spirit, we include a short tutorial that simulates fluorescence anisotropy. Furthermore, all of the code to generate the simulations in this work is available on GitHub. For faster performance, a GPU-accelerated version is also available.

Case Study 1: Can we measure tumbling cheaply?

Tumbling measurements are often associated with high-end, expensive microscopes and careful selection of fluorophores. As rapid COVID tests and pregnancy tests demonstrate, sophisticated technology can become staggeringly impactful to society if it becomes sufficiently cheap. Therefore, we choose to explore the space of simple hardware and universal photophysics. The core hardware components we employ in this case study (focused laser, photodiode) are minimal and cheap; for reference, they are contained within CD players. On the sample side, we require only that the target is labeled with a fluorophore that can be shelved into a long-lived, non-emissive state by illumination with light. Photobleaching, for example, is a universal mechanism for shelving fluorophores following illumination. Some fluorophores display additional shelving photophysics; for example, many fluorophores can be shelved into microsecond or millisecond-lived triplet states [e.g. Schönle 2014, Peng 2021], and reversible switchable fluorescent proteins (rsFPs) can be shelved into an inactive state [Zhou 2013].

Concretely, we simulate a continuous linearly polarized beam, which illuminates a sample while two detectors integrate polarization of the output fluorescence (Figure 3 with `Shelving Only` selected). In our model, illumination causes shelving by photobleaching via a triplet intermediate state [Ludvikova 2023], but the essence of this result does not depend on the details of the shelving mechanism. Our time-integrated approach differs from previous implementations of tumbling with photobleaching, which required an intense polarized light pulse to bleach out a subset of the ground state orientations [e.g. Smith 1981, Velez 1988], followed by lower intensity illumination to track the scrambling of this "etched" ground state distribution. Unlike that approach, we do not require rapid photobleaching kinetics or sub-microsecond detector time resolution, which might be difficult to achieve with diverse fluorophores and with low-cost hardware.

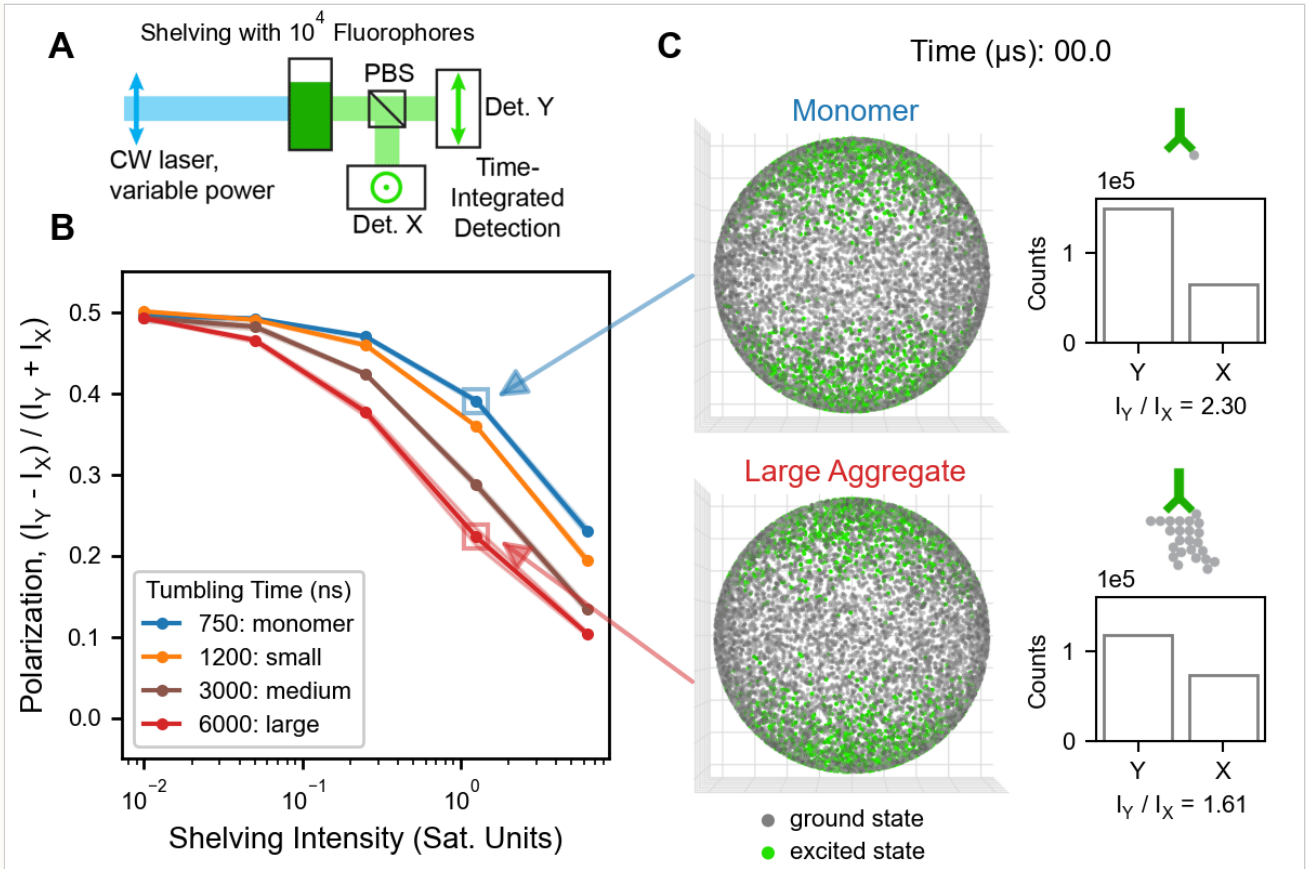

Photophysics: Shelving Only

Figure 3: Power variations in a shelving beam reveal size with minimal hardware.
(A) Cartoon of the simulated experiment, with a laser (light blue) illuminating a solution (e.g. in a cuvette). Two detectors record the fluorescence emission (I_X and I_Y, green) after a polarizing beam splitter (PBS). `Shelving Only` simulates photobleaching, but triplet generation or off-switching of an rsFP could be readily substituted with near-identical results. Similarly, `Shelving and Unshelving` simulates off- and on-switching of an rsFP but could just as easily be triplet shelving and triggering. For `Shelving and Unshelving`, an unshelving laser (dark blue) with intensity 0.01 saturation (sat.) units was fired concurrently with the shelving laser (light blue). **(B)** Polarization of the time-integrated fluorescence emission as it varies with the intensity of the shelving beam. Signal was integrated over 100 μs. Points are means of 3 replicates, with shaded areas indicating ± standard deviation. **(C)** Time course of a measurement with shelving intensity of 1.25 sat. units. Points on a sphere indicate molecular orientations, with the shelving beam polarized in the up/down direction. Bar graphs indicate accumulating signal on the detectors. The slower rotation of the large aggregate increases etching of the ground state orientation distribution (gray) and reduces the polarization.

It is useful to imagine the time course of this shelving experiment (Figure 3C, Option `Shelving Only`), even though the final signal is time-integrated. For a fully immobile population, high laser intensity will strongly etch the orientation distribution of the ground state population. Initially, emission will be mostly parallel to the excitation beam, but as shelving progresses, very few ground state fluorophores will remain parallel to the excitation beam. The remaining fluorophores' orientations are enriched perpendicular to the excitation beam, so the detected emissions are increasingly likely to be in the perpendicular channel (lower polarization). By contrast, a population that is rotating rapidly will repopulate the parallel channel and retain high polarization over time, even as the total fluorescence decreases. The relative rates of shelving and rotation determine the integrated polarization. By varying the laser power in successive measurements one can vary the rate of shelving and obtain a spectrum.

If we are using a reversible shelving process such as rsFP off-switching or triplet generation, we have the option of "unshelving," or bringing the fluorophores from the non-emissive state back to an emissive one, with another color of light. We can imagine this as either a two-step or a one-step process. In the two-step version, the unshelving beam would be used to regenerate the sample after a measurement with the shelving beam. Conceptually, this scheme is the same as `Shelving Only`, with the added convenience of not having to find another region in the sample for successive measurements. In a one-step scheme, the shelving and unshelving beams illuminate the sample concurrently (Figure 3, option `Shelving and Unshelving`). The unshelving beam, polarized perpendicularly to the shelving beam, continuously regenerates the sample. We predict that this configuration will yield clear signals even for low numbers of fluorophores (100 total in the simulation, equivalent to a concentration of 2.5 nM in a 5 μm diameter spherical focal volume).

This intensity variation scheme could be applied, for example, with commercially available antibodies to determine level of aggregation of the antibody’s target in blood or cerebrospinal fluid. It also could be deployed as an alternative to the common co-immunoprecipitation or “pulldown” assay to determine whether a labeled target protein is bound to any additional molecules in a mixture.

Case Study 2: Can we measure tumbling at billions of voxels per second?

To study spatially heterogeneous samples (e.g. cells, tissues), we would like to map protein-protein interactions across the entire sample. For live samples, we also want to reveal the

temporal dynamics of these interactions. State-of-the-art lightsheet microscopes [Millett-Sikking 2019] can measure fluorescence intensity in 3D at video rate. What would it take to incorporate tumbling as an additional channel of information on such a microscope?

A critical component of fast imaging systems is camera-based detection, where signal from a 2D plane is recorded in parallel. A standard scientific camera can acquire an image on millisecond timescales, but tumbling involves nanosecond- or microsecond-scale dynamics. To access these shorter timescales, fluorescence anisotropy is typically recorded with a single pixel detector that counts individual photons with sub-nanosecond time resolution [Lakowicz 2006, Volpato 2023, Lu 2023]. Images are then (very slowly) formed by raster scanning a point through the sample. Parallelized, multipixel versions of these detectors are in development [McShane 2022], but the photon count rates they support are orders of magnitude lower than modern cameras.

With current camera technology, a “pump-probe” imaging scheme could allow imaging an entire field of view simultaneously. Time resolution is encoded by a variable delay between pump and probe laser pulses; each camera exposure records a single delay (Figure 4). The 7 delays we simulate yield excellent prediction of intermediate delays, suggesting that a modest number of delays is sufficient to capture tumbling dynamics. Critically, such an approach would be compatible with both widefield and lightsheet microscopes.

On the fluorophore side, we need a long-lived state (e.g. an rsFP or a triplet) that can be triggered to emit by a probe beam. "Triggered triplets" (also known as optically activated delayed fluorescence) refers to millisecond-lived triplet states that can emit prompt fluorescence when excited with far-red light [Peng 2021]. Triplets can be generated from the excited singlet, leading to a convenient pulse scheme where a pump pulse at the traditional absorption wavelength (e.g. 488 nm for fluorescein) is followed by a far-red probe pulse [Demissie 2020]. Recently, it was experimentally reported that the triggered triplet signal is compatible with tumbling measurements [Lu 2023]. Here, we focus on triplets rather than rsFPs because they don't have a microsecond-scale dead time following the pump beam, allowing access to nanosecond timescales.

We simulate a linearly polarized pump pulse and an orthogonally polarized probe (trigger) pulse (Figure 4). Two gated but otherwise standard cameras record fluorescence following a polarizing beamsplitter. The pump beam generates triplets that are partially aligned with its polarization and therefore partially anti-aligned with the probe beam's polarization. For bookkeeping

purposes, we choose the pump polarization as the reference direction. As scrambling occurs and the partial alignment with the pump polarization is lost, the emission polarization becomes more negative (orthogonal to the pump). A fully scrambled population will give a polarization of -0.5, although saturation in the probe beam can reduce the magnitude of the polarization.

Using this pulse scheme, we simulate a sample of labeled protein with three binding states: unbound, bound to a small partner, or bound to a large partner. Our results show distinguishable tumbling curves for all three binding states. Importantly, the tumbling curve of a mixture of the unbound and large states is also distinguishable from that of a binding partner of intermediate mass; we anticipate such mixtures will be the norm in a real sample. One could imagine applying this architecture to many biological systems, e.g.:

- Assembly of multipart protein machines, e.g. the V-ATPase [Forgac 1998]
- Recruitment of downstream effectors of receptor tyrosine kinases to the membrane [Lemmon 2010]
- Transcription factor dimerization and binding to DNA [Amoutzias 2008]

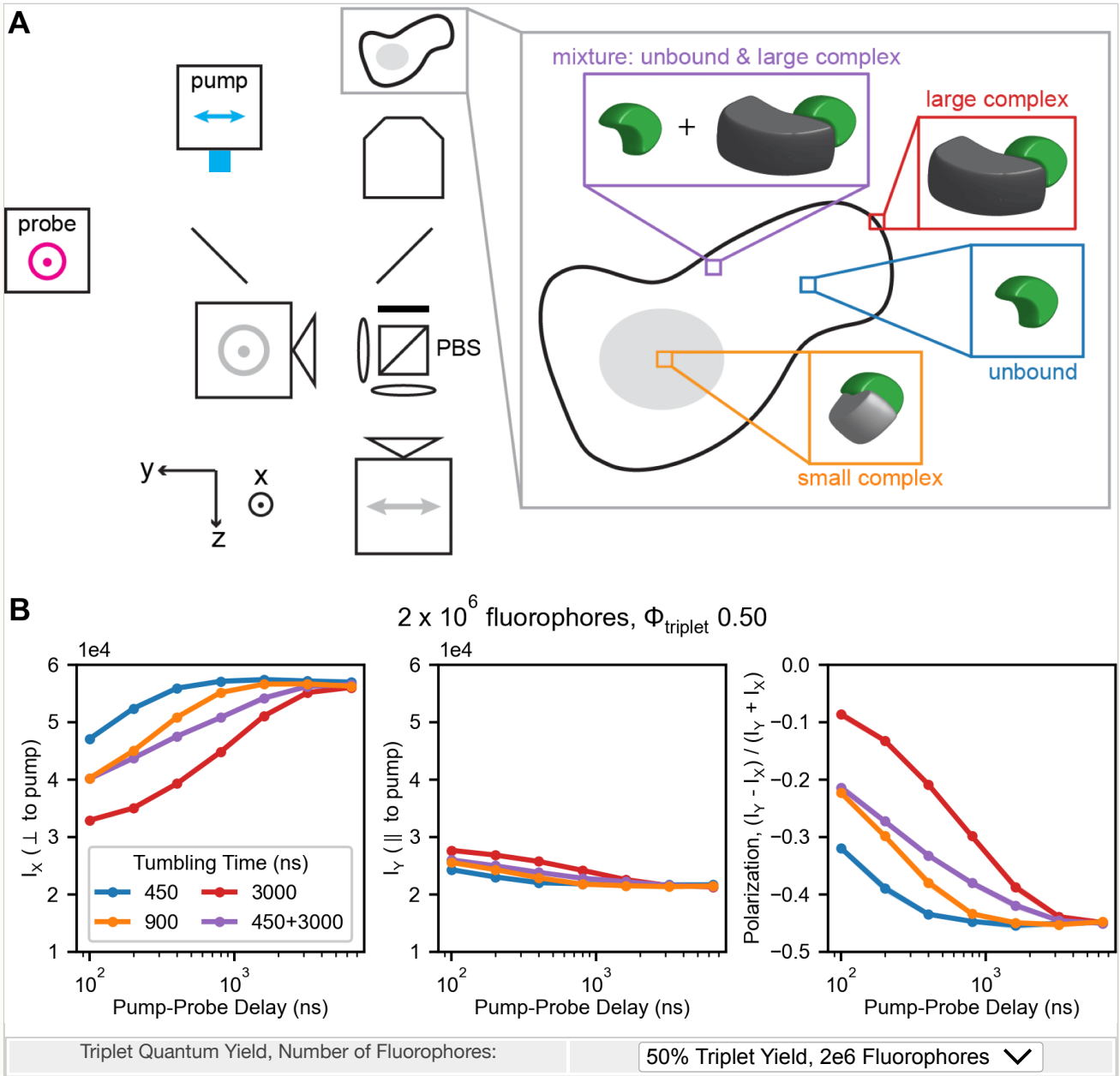

Triplet Quantum Yield, Number of Fluorophores: 50% Triplet Yield, 2e6 Fluorophores

Figure 4. Pump-probe measurements with triggered emitters allow massively parallel tumbling measurements.

(A) Schematic of a pump-probe simulation with triggered triplets. The pump pulse (blue) generates fluorescence (green) in the sample. Some of these fluorescent molecules convert to triplets (faint pink), which, after a variable delay, are triggered to fluoresce (green) by the probe beam (pink). A fast shutter separates signal from the pump and probe pulses. A polarizing beamsplitter followed by two cameras records the polarized fluorescence at all points in the image. A sequence of delays is captured by successive images. Inset from sample shows a cartoon representation of how tumbling times could correspond to spatially compartmentalized binding events within a cell. **(B)** Intensities in the X and Y detector channels (I_X, I_Y) and resulting polarization for tumbling times of 450 ("unbound"), 900 ("small complex"), and 3000 ns ("large complex"), as well as an equal part mixture of 450 and 3000 ns tumbling times. Pump and probe pulses were 50 ns in duration with intensity 0.25 saturation units. Points indicate means of 6 replicate simulations, with shaded areas indicating ± standard deviation.

The primary drawback of triggered triplets relative to rsFPs is the low number of photons produced per molecule. The quantum yield of triplet generation in existing fluorescent proteins is ≈1% [Peng 2021]; once triggered, a triplet emits at most one photon. To obtain low-variance tumbling curves, we simulate 50% triplet quantum yield and/or 10^5-10^6 molecules. In a real sample, the number of molecules available will be constrained by the expression level of the target protein. A cell contains ≈10^6 total proteins per cubic micron [Milo 2013]; for targets other than the most abundant, we are unlikely to have more than ≈10^3 fluorophores per cubic micron. Therefore, for many proteins of interest, we will likely be starved for photons. To circumvent this, we can bin triplet images either in space or in time (by accumulating successive pump-probe cycles) to obtain enough signal to resolve binding states. The effects of triplet quantum yield and number of molecules can be explored through the drop-down options in Figure 4.

Case Study 3: Can we measure tumbling across millions of conditions in an hour?

Pooled assays involving many conditions, e.g. large genetic perturbation libraries, are powerful when we don't have strong prior knowledge of a biological system and want to discover the relevant pieces. For these experiments, spatial resolution isn't required, but the ability to interrogate many cells in quick succession is critical. Conveniently, pump-probe tumbling schemes with triggered triplets (Figure 4) are also compatible with flow cytometry (Figure 5), dramatically increasing throughput. Such an approach could characterize the effect of mutagenesis or knockout on protein-protein interactions at scale.

A pump-probe excitation scheme in a flow cytometer could be achieved either via physical spacing of the pump and probe laser along the object's path or via pulsed lasers and time-gated detection. At a linear flow rate of 10 m/s [Kalb 2017], two 10 μm wide laser spots separated by 50 μm would produce a 5 μs delay; a sequence of beam spacings produces a sequence of delays. Flow cytometers often incorporate additional spectral channels in this manner, so this proposal requires minimal modification of existing systems. For time delays shorter than 1 μs, pump-probe pulse pairs could also be delivered within the dwell time of the cell in a particular focused spot, provided that the detector was able to gate out any emission generated by the pump pulse.

A key difference between this approach and a camera-based system (Figure 4) is that it would be inconvenient to wait milliseconds for untriggered triplets to naturally decay. With flow rates fast enough to achieve microsecond delays, millisecond wait times in between measurements

would involve long additional fluidic lines. To improve successive pump-probe sequences, we simulate a circularly polarized probe beam (Figure 5 with `Circular` selected), which reduces buildup of untriggered triplets between cycles versus a linearly polarized probe beam (Figure 5 with `Linear` selected).

As with the simulation in Figure 4, three different size targets produce three distinguishable tumbling curves (Figure 5). Because it does not require spatial resolution, a flow cytometer can more easily compensate for the low triplet quantum yields of existing FPs than a camera-based system can. Here, we simulate 1% triplet quantum yield and 10^6 fluorophores, which is attainable within a single mammalian cell using existing fluorescent proteins and a target that makes up 0.01-0.1% of the proteome [Milo 2013].

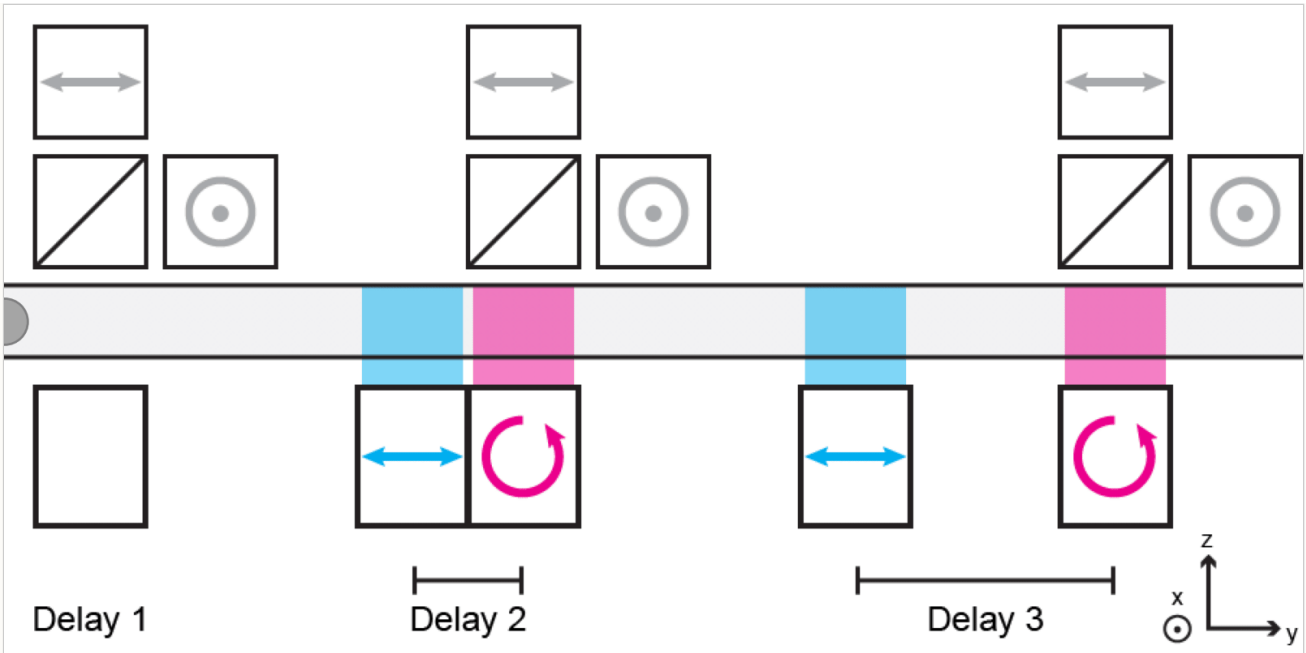

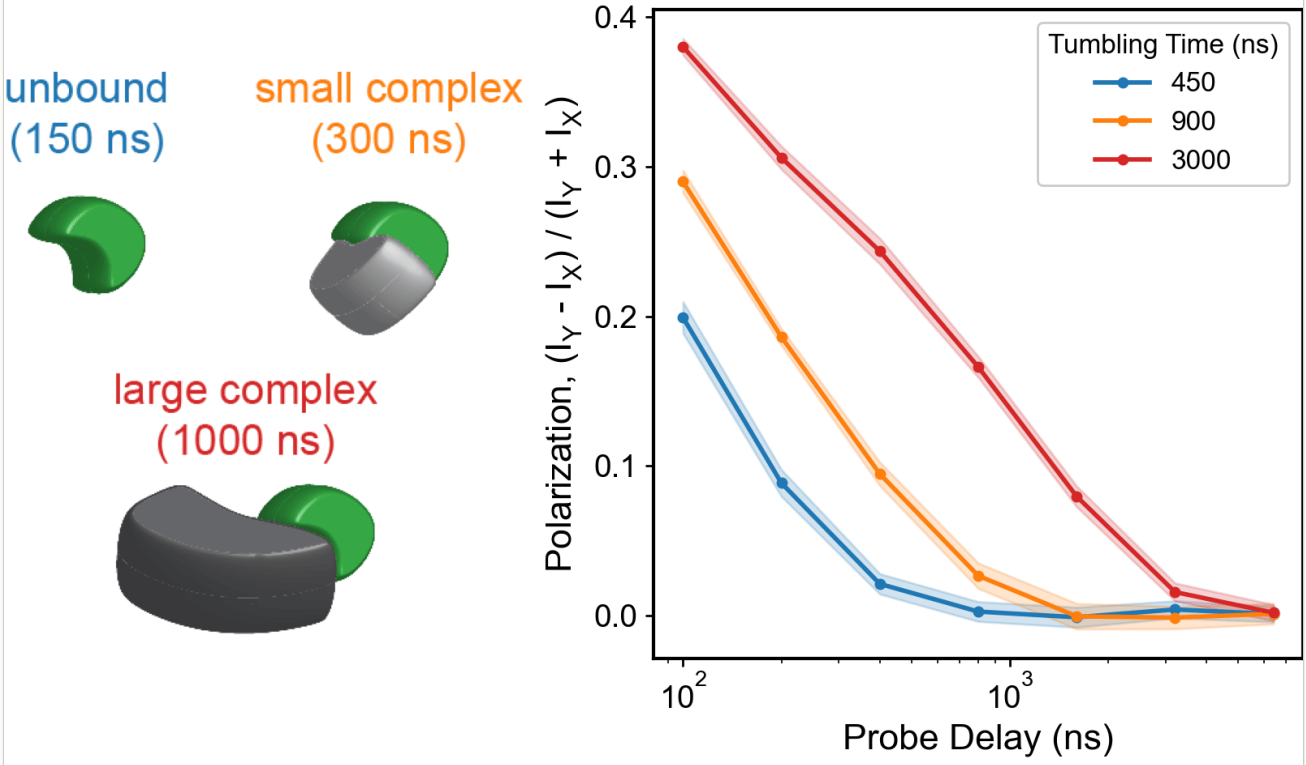

Probe Polarization: Circular (XY plane)

Figure 5. Pump-probe based tumbling measurements are compatible with flow cytometry.
Top: Cartoon of a cell in a flow cytometer, interrogated at different tumbling delays as it proceeds through the flow cell. Triggered triplet photophysics are illustrated (green=singlet, pink=triplet), generated by a linearly polarized pump beam (blue) and a circularly (XY plane) or linearly (X) polarized probe beam (pink). A short delay with pulsed pump and probe in one location is shown on the left, with two spatially generated delays with continuous pump and probe illumination in the middle and right. **Bottom left:** Cartoon of how binding states could correspond to rotational diffusion times. **Bottom right:** Evolution of the polarization signal versus delay for samples of different tumbling times. Points are means of 12 replicate simulations, each with 10^6 fluorophores and 1% triplet yield. Shaded areas are ± standard deviation. The pink box highlights the delay that the cartoon would be currently measuring.

Case Study 4: Can we measure tumbling on an existing commercial instrument?

Most biologists buy imaging systems rather than build them, relying on vendors and distributors to get the next generation of technology into their labs. As a result, the impact of new techniques is often delayed, as the commercialization process can take years. We could potentially shortcut this process, as the necessary hardware is already available on many commercial confocal instruments. Confocal illumination can deliver the intensities required for case study 1, and the temporal control over lasers and detectors required for the pump-probe style measurements described in case studies 2 and 3 exists on a subset of these instruments. Therefore, a sizable population of instruments capable of measuring tumbling of protein complexes is already deployed and "just" needs a software update. To motivate vendors to support this, we used our unmodified, 8-year-old Leica SP8 confocal microscope to make a pump-probe tumbling measurement.

Our SP8 confocal microscope contains many of the components that [Lu 2023] used to measure triplet triggering and tumbling in mVenus. In addition to a visible laser to generate triplets, we have a far-red or infrared laser to trigger the triplets. Our 775 nm laser was not exactly the reported wavelength, but triplet absorption spectra are typically broad [Ludvikova 2023]. Its donut-shaped focused spot (originally intended for STED) is suboptimal but manageable for the triggering beam. Conveniently, our visible and 775 nm lasers (with the quarter-wave plate removed) are then linearly polarized in orthogonal directions. To measure emission polarization, our system has a polarizing beamsplitter and two detectors on the back port, but these measurements could also be made with the built-in detectors and polarizer. Finally, we need a way to separate the prompt fluorescence and triggered triplet emission in time. Instrument software prevented us from flexibly controlling either the visible laser repetition rate or the AOTF, so we resorted to using successive sweeps of the resonant scanner to interrogate the sample at 60 µs intervals. To extract the data, we used a custom parser for the raw time-tagged photon stream. This approach is substantially suboptimal relative to case study 2, but its existence and accessibility on current instruments makes it compelling.

Because instrument software prevented us from accessing timescales shorter than microseconds, we chose to measure FP-labeled beads instead of protein targets. Triplet triggering has previously been demonstrated for mVenus [Peng 2021]; we wanted to replicate this and also investigate whether it generalized to the commonly used fluorescent proteins mEGFP [Zacharias 2002] and mScarlet [Bindels 2017]. We used a range of bead samples at

known sizes (40, 60, 100, and 200 nm diameter) to benchmark our measurements against simulation. We adsorbed purified FPs to the surface of these beads, optimizing the protocol to minimize bead aggregation and residual free protein (Figure S2, Figure S3).

We then investigated the triggered triplet signal, which we were pleased to find in both mEGFP and mScarlet. 775 nm illumination (400 μW average power) produced fluorescence if and only if the sample was previously illuminated at 488 nm (mEGFP, mVenus) or 561 nm (mScarlet), suggesting that the initial pulse generated a long-lived triggerable state (i.e. a triplet, Figure S1). mVenus's triplet lifetime was reported to be approximately 1 ms [Peng 2021]; we replicate this and observe a similar triplet lifetime for mScarlet (Figure S4). Following 775 nm illumination, the triggered fluorescence is short-lived, with a lifetime similar to that of the prompt fluorescence from the singlet (≈2 ns, Figure S5, Figure S6). These characteristics are consistent with triggered fluorescence from the triplet state.

When we analyze how the polarization of the triggered triplet signal changes over time, we observe distinct tumbling decays from the 4 bead diameters (Figure 6). Our experimental results qualitatively match simulations, with similar time dynamics but a reduction in the magnitude of the polarization changes. A substantial part of this reduction in magnitude results from our high numerical aperture (NA) objective. We anticipate that using a lower NA objective lens would enhance the measured polarization changes, at the expense of some collection efficiency.

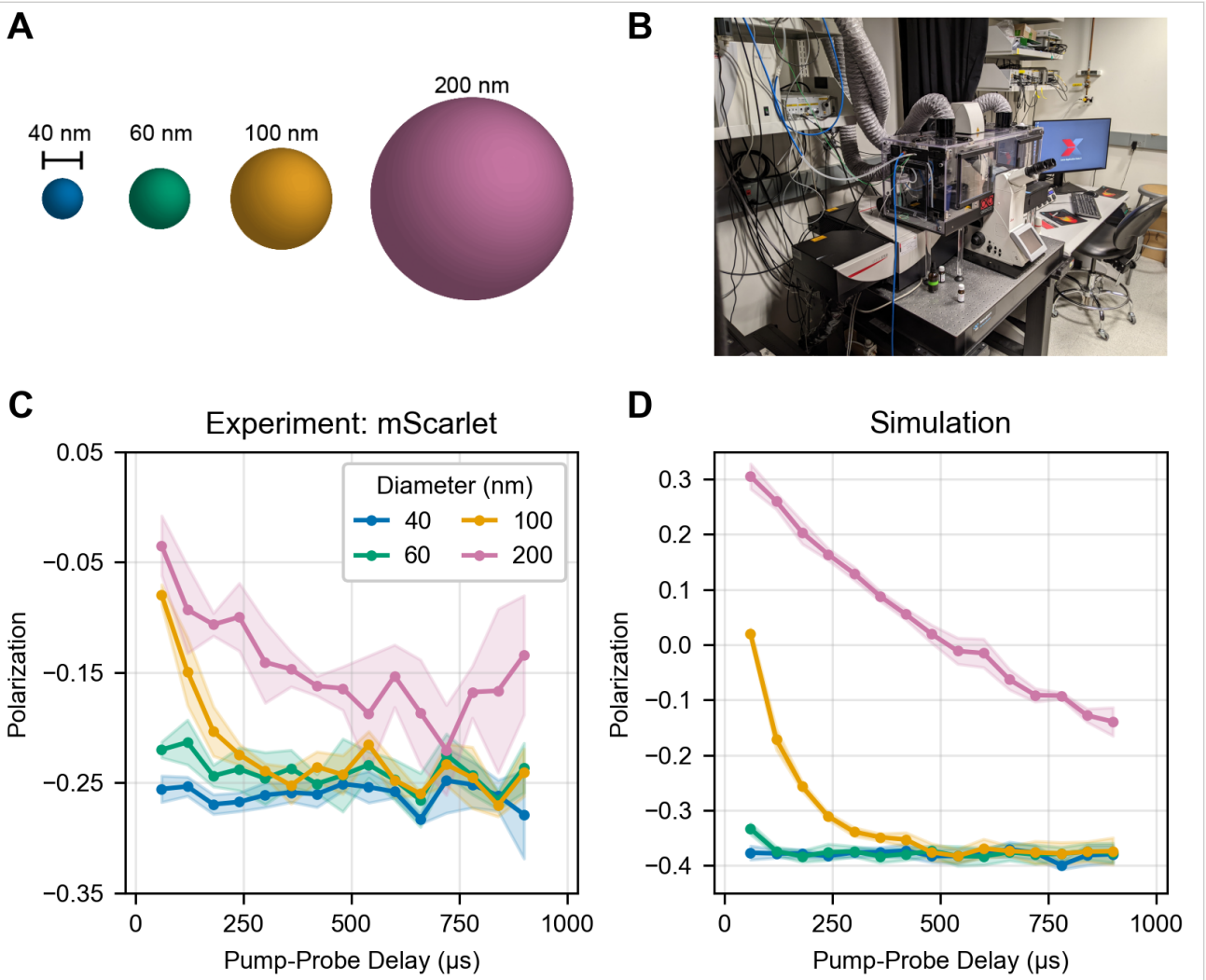

Figure 6. Tumbling of nanometer-scale beads can be measured on a commercially available microscope via triplet triggering.

(A) Cartoon representation of bead samples used in this experiment and simulation. **(B)** Photograph of the Leica SP8 used for these experiments. **(C)** Experimental tumbling data acquired on FP-labeled beads. Drop-down menu toggles between mScarlet and mVenus recordings. Pulse scheme and instrumentation are described in Figure S1. **(D)** Simulation of (C) with 10^6 molecules and saturating pump (16 pulses of intensity 2) and probe (16 pulses of intensity 0.25) illumination, matching the 200 ns dwell time and 80 MHz repetition rate of the experimental laser. Simulated intensities were approximately matched to experiment. In (C) and (D), points are means, with shaded areas indicating ± standard deviation of n=3 (experiment) or n=6 (simulation) replicates.

Outlook

If instruments capable of measuring tumbling on protein-relevant timescales were readily available to biologists, we believe they would become the tools of choice for revealing protein-protein interactions. However, a few roadblocks remain before their full potential can be realized, particularly in fluorophore engineering and data analysis.

In this work, we have concerned ourselves only with perfectly rigid labels, where the fluorophore and the target move as one. Typical linkers for tagging proteins with FPs are flexible, allowing some movement of the fluorophore label independent of the target, which scrambles polarization information [Fooksman 2007, Volpato 2023]. The resulting hindered tumbling of the fluorophore could be dealt with at the data analysis level, but in many cases, it may be prudent to re-engineer the linkers so that the fluorophore tumbling more accurately reflects tumbling of the target. To this end, development of modular, rigid tagging strategies would simplify the onboarding of new proteins of interest.

Existing triggerable triplets and rsFPs are usable for tumbling measurements [Volpato 2023, Lu 2023], but they deviate from the "ideal" triggerable emitter. The key shortcoming of triggerable triplets in existing fluorescent proteins is their low quantum yield. Small-molecule fluorophores with high yields of triggerable triplets exist [Demissie 2020], but they are highly phototoxic. Development of genetically encoded labels with high triplet yields while maintaining their low triplet reactivities [Byrdin 2018] would enhance signal in tumbling measurements. Much remains unknown about the mechanism of triplet triggering, and a deeper understanding of the fundamental photophysics would aid engineering efforts. In rsFP activation, the fluorophore goes through a microsecond-lived dark state, erasing tumbling information in a critical size window. In addition, rsFP activation and excitation absorption dipoles (and likely triplet generation and triggering dipoles) are not parallel, blurring the orientation distribution and reducing the dynamic range of polarization. Optimizing these properties would make rsFPs and triplets more effective in protein-protein interaction studies.

In this work, we developed a forward model for predicting tumbling measurements from target size, demonstrating that different target sizes produce obviously distinct tumbling curves. In some experimental scenarios, stating that two samples have distinct tumbling curves may be sufficient (e.g. "the drug disrupted the protein complex"). Taking it a step further, an inverse model would infer a spectrum of sizes from the tumbling decay of a tagged protein, ideally

modeling protein tumbling in diverse conditions (in solution, membrane bound, changing conformation, etc.). As inverse models emerge, they will not only enable such analyses but also help refine measurement schemes, clarifying which information is preserved or erased by a given hardware configuration.

Most protein-protein interaction assays are confirmatory: the experimenter suspects that two proteins interact and they want to verify this. An idealized tumbling experiment goes far beyond this: it's a discovery engine that, from a single labeled protein, could report the sizes of all interaction partners, resolved across space and time. Such a tool, when fully realized, will bring us ever closer to understanding the cascades of molecular interactions that underlie life.

Acknowledgements

We thank Andrea Volpato, Ilaria Testa, Alfred Millett-Sikking, and James Manton for thoughtful advice and feedback. We thank Kayley Hake, Martin Mullis, and Alyssa Kaiser for brainstorming and feedback on the tumbling animation. We thank the many excellent scientists at Calico Life Sciences LLC for providing stimulating discussions throughout this project.

Author Contribution Statement

J.R.L.D. contributed to conceptualization of the project, ran simulations, designed and performed experiments, interpreted data, and wrote the manuscript. A.E.Y.T.L. contributed to conceptualization of the project, ran simulations, and interpreted data. R.F.H. performed experiments. L.W. made the tumbling animation (Figure 1). M.I. performed experiments and contributed to conceptualization of the project. A.G.Y. wrote the fluorophore simulation code and contributed to conceptualization of the project and writing of the manuscript.

Funding and Conflict of Interest Statement

This project was supported by Calico Life Sciences LLC. M.I. and A.G.Y. are inventors on a patent related to tumbling with long-lived states and crescent depletion (US Patent US20210247315A1), and J.R.L.D., M.I., and A.G.Y. have filed a patent on triggered triplets for tumbling.

Open-source software

As always, our work here depends critically on the open-source software community. Among our crucial dependencies (listed with version numbers used in this work):

- Python (version 3.9.9)
- Numpy (version 1.21.4) [Harris 2020]
- Scipy (version 1.7.2) [Virtanen 2020]
- Pandas (version 1.5.3) [pandas-dev 2020]
- Matplotlib (version 3.7.1)
- FFmpeg

We sincerely thank the authors of these projects for enabling our work.

Appendix

Methods and additional discussion can be found in the Appendix, which is also referenced via hyperlinks throughout this article.

References

1. [Lakowicz 2006] Principles of Fluorescence Spectroscopy; J. R. Lakowicz; ISBN 978-0-387-31278-1 (2006) https://doi.org/10.1007/978-0-387-46312-4
2. [York 2019] System and Method for Inferring Protein Binding; A. G. York, M. del Mar Ingaramo; US Patent US20210247315A1 (2019) https://patents.google.com/patent/US20210247315A1
3. [Weber 1952] Polarization of the fluorescence of macromolecules. 1. Theory and experimental method; G. Weber; Biochem J., 51, 2, 145–155 (1952) https://doi.org/10.1042/bj0510145
4. [Los 2008] HaloTag: a novel protein labeling technology for cell imaging and protein analysis; G.V. Los, L.P. Encell, M.G. McDougall, D.D. Hartzell, N. Karassina, C. Zimprich, M.G. Wood, R. Learish, R.F. Ohana, M. Urh, D. Simpson, J. Mendez, K. Zimmerman, P. Otto, G. Vidugiris, J. Zhu, A. Darzins, D.H. Klaubert, R.F. Bulleit, K.V. Wood; ACS Chemical Biology, 20, 3(6), 373-382 (2008) https://doi.org/10.1021/cb800025k
5. [Juillerat 2003] Directed Evolution of O6-Alkylguanine-DNA Alkyltransferase for Efficient Labeling of Fusion Proteins with Small Molecules In Vivo; A. Juillerat, T. Gronemeyer, A. Keppler, S. Gendreizeg, H. Pick, H. Vogel, K. Johnsson; Cell Chemical Biology, 10, 4, 313-317 (2003) https://doi.org/10.1016/S1074-5521(03)00068-1

6. [Netzer 1998] Protein folding in the cytosol: chaperonin-dependent and -independent mechanisms; W. J. Netzer, F. U. Hartl; Trends in Biochemical Sciences, 23, 2, 68-73 (1998) https://doi.org/10.1016/S0968-0004(97)01171-7
7. [Austin 1979] Rotational diffusion of cell surface components by time-resolved phosphorescence anisotropy; R. H. Austin, S. S. Chan, T. M. Jovin; Proceedings of the National Academy of Sciences, 76, 11, 5660-5654 (1979) https://doi.org/10.1073/pnas.76.11.5650
8. [Moore 1979] Phosphorescence depolarization and the measurement of rotational motion of proteins in membranes; C. Moore, D. Boxer, P. Garland; FEBS Letters, 108, 1, 161-166 (1979) https://doi.org/10.1016/0014-5793(79)81200-4
9. [Smith 1981] Measurement of rotational motion in membranes using fluorescence recovery after photobleaching; L.M. Smith, R.M. Weis, H.M. McConnell; Biophysical Journal, 36, 1, 73-91 (1981) https://doi.org/10.1016/S0006-3495(81)84717-0
10. [Velez 1988] Polarized fluorescence photobleaching recovery for measuring rotational diffusion in solutions and membranes; M. Velez, D. Axelrod; Biophysical Journal, 53, 4, 575-591 (1988) https://doi.org/10.1016/S0006-3495(88)83137-0
11. [Volpato 2023] Extending fluorescence anisotropy to large complexes using reversibly switchable proteins; A. Volpato, D. Ollech, J. Alvelid, M. Damenti, B. Müller, A. G. York, M. Ingaramo, I. Testa; Nature Biotechnology, 41, 552–559 (2023) https://doi.org/10.1038/s41587-022-01489-7
12. [Lu 2023] Sequential Two-Photon Delayed Fluorescence Anisotropy for Macromolecular Size Determination; Y.-H. Lu, M. C. Jenkins, K. G. Richardson, S. Palui, M. S. Islam, J. Tripathy, M. G. Finn, R. M. Dickson; J. Phys. Chem. B, 127, 17, 3861–3869 (2023) https://doi.org/10.1021/acs.jpcb.3c01236
13. [Felker 1986] Rephasing of collisionless molecular rotational coherence in large molecules; P.M. Felker, J.S. Baskin, A.H. Zewail, J. Phys. Chem. 90, 5, 724-728 (1986) https://doi.org/10.1021/j100277a006
14. [Ghosh 2013] A "Gaussian" for diffusion on the sphere; A. Ghosh, J. Samuel, arXiv:1303.1278v1 (2013) https://doi.org/10.48550/arXiv.1303.1278
15. [Myšková 2020] Directionality of light absorption and emission in representative fluorescent proteins; J. Myšková, O. Rybakova, J. Brynda, P. Khoroshyy, A. Bondar, J. Lazar; Proceedings of the National Academy of Sciences, 117, 51, 32395-32401 (2020) https://doi.org/10.1073/pnas.2017379117
16. [Yadav 2015] Real-Time Monitoring of Chromophore Isomerization and Deprotonation during the Photoactivation of the Fluorescent Protein Dronpa; D. Yadav, F. Lacombat, N. Dozova, F.

Rappaport, P. Plaza, A. Espagne; J. Phys. Chem. B, 119, 6, 2404-2414 (2015) https://doi.org/10.1021/jp507094f

17. [Lettinga 2000] Phosphorescence and fluorescence characterization of fluorescein derivatives immobilized in various polymer matrices; M.P. Lettinga, H. Zuilhof, M.A.M.J. van Zandvoort; Phys. Chem. Chem. Phys., 2, 3697-3707 (2000) https://doi.org/10.1039/a909707d
18. [Schönle 2014] Monitoring triplet state dynamics with fluorescence correlation spectroscopy: Bias and correction; A. Schönle, C. Von Middendorff, C. Ringemann, S.W. Hell, C. Eggeling, Microscopy Research and Technique, 77, 528-536. (2014) https://doi.org/10.1002/jemt.22368
19. [Peng 2021] Optically Modulated and Optically Activated Delayed Fluorescent Proteins through Dark State Engineering; B. Peng, R. Dikdan, S. E. Hill, A. C. Patterson-Orazem, R. L. Lieberman, C. J. Fahrni, R. M. Dickson; J Phys Chem B, 125, 20, 5200-5209 (2021) https://doi.org/10.1021/acs.jpcb.1c00649
20. [Zhou 2013] Photoswitchable Fluorescent Proteins: Ten Years of Colorful Chemistry and Exciting Applications; X. X. Zhou, M. Z. Lin, 17, 4, 682–690. (2013) https://doi.org/10.1016/j.cbpa.2013.05.031
21. [Ludvikova 2023] Near-infrared co-illumination of fluorescent proteins reduces photobleaching and phototoxicity; L. Ludvikova, E. Simon, M. Deygas, T. Panier, M.-A. Plamont, J. Ollion, A. Tebo, M. Piel, L. Jullien, L. Robert, T. Le Saux, A. Espagne; Nature Biotechnology (2023) https://doi.org/10.1038/s41587-023-01893-7
22. [Millett-Sikking 2019] High NA single-objective light-sheet; A. Millett-Sikking, K. M. Dean, R. Fiolka, A. Fardad, L. Whitehead, A. G. York; Zenodo. (2019) https://doi.org/10.5281/zenodo.3244420
23. [McShane 2022] High resolution TCSPC imaging of diffuse light with a one-dimensional SPAD array scanning system; AE. P. McShane, H. K. Chandrasekharan, A. Kufcsák, N. Finlayson, A. T. Erdogan, R. K. Henderson, K. Dhaliwal, R. R. Thomson, M. G. Tanner; Optics Express, 30, 15, 27926-27937 (2022) https://doi.org/10.1364/OE.461334
24. [Demissie 2020] Triplet Shelving in Fluorescein and Its Derivatives Provides Delayed, Background-Free Fluorescence Detection; A. A. Demissie, R. M. Dickson; J Phys Chem A 124, 7, 1437-1443 (2020) https://doi.org/10.1021/acs.jpca.9b11040
25. [Forgac 1998] Structure, function and regulation of the vacuolar (H+)-ATPases; M. Forgac; FEBS Letters, 440, 3, 258-263 (1998) https://doi.org/10.1016/S0014-5793(98)01425-2
26. [Lemmon 2010] Cell signaling by receptor-tyrosine kinases; M. A. Lemmon, J. Schlessinger; Cell, 141, 7, 1117–1134 (2010) https://doi.org/10.1016/j.cell.2010.06.011

27. [Amoutzias 2008] Choose your partners: dimerization in eukaryotic transcription factors; G. D. Amoutzias, D. L. Robertson, Y. Van de Peer, S. G. Oliver; Trends in Biochemical Sciences, 33, 5, 220-229 (2008) https://doi.org/10.1016/j.tibs.2008.02.002
28. [Milo 2013] What is the total number of protein molecules per cell volume? A call to rethink some published values; R. Milo; Bioessays, 35, 12, 1050-1055 (2013) https://doi.org/10.1002/bies.201300066
29. [Kalb 2017] Line Focused Optical Excitation of Parallel Acoustic Focused Sample Streams for High Volumetric and Analytical Rate Flow Cytometry; D. M. Kalb, F. A. Fencl, T. A. Woods, A. Swanson, G. C. Maestas, J. J. Juárez, B. S. Edwards, A. P. Shreve, S. W. Graves; Anal. Chem., 89, 18, 9967-9975 (2017) https://doi.org/10.1021/acs.analchem.7b02319
30. [Zacharias 2002] Partitioning of Lipid-Modified Monomeric GFPs into Membrane Microdomains of Live Cells; D.A. Zacharias, J.D. Violin, A.C. Newton, R.Y. Tsien; Science 296, 5569, 913-916 (2002) http://doi.org/10.1126/science.1068539
31. [Bindels 2017] mScarlet: a bright monomeric red fluorescent protein for cellular imaging; D. S. Bindels, L. Haarbosch, L. van Weeren, M. Postma, K. E. Wiese, M. Mastop, S. Aumonier, G. Gotthard, A. Royant, M. A. Hink, T. W. J. Gadella Jr; Nature Methods 14, 53-56 (2017) http://doi.org/10.1038/nmeth.4074
32. [Fooksman 2007] Measuring Rotational Diffusion of MHC Class I on Live Cells by Polarized FPR; D. R. Fooksman, M. Edidin, B. G. Barisas; Biophys Chem, 130, 1-2, 10-16 (2007) https://doi.org/10.1016/j.bpc.2007.06.013
33. [Byrdin 2018] A Long-Lived Triplet State Is the Entrance Gateway to Oxidative Photochemistry in Green Fluorescent Proteins; M. Byrdin, C. Duan, D. Bourgeois, K. Brettel; Journal of the American Chemical Society 140, 8, 2897-2905 (2018) https://doi.org/10.1021/jacs.7b12755
34. [Harris 2020] Array programming with NumPy; Charles R. Harris, K. Jarrod Millman, Stéfan J. van der Walt, Ralf Gommers, Pauli Virtanen, David Cournapeau, Eric Wieser, Julian Taylor, Sebastian Berg, Nathaniel J. Smith, Robert Kern, Matti Picus, Stephan Hoyer, Marten H. van Kerkwijk, Matthew Brett, Allan Haldane, Jaime Fernández del Río, Mark Wiebe, Pearu Peterson, Pierre Gérard-Marchant, Kevin Sheppard, Tyler Reddy, Warren Weckesser, Hameer Abbasi, Christoph Gohlke & Travis E. Oliphant; Nature 585, 357–362 (2020) http://doi.org/10.1038/s41586-020-2649-2
35. [Virtanen 2020] SciPy 1.0: Fundamental Algorithms for Scientific Computing in Python; Pauli Virtanen, Ralf Gommers, Travis E. Oliphant, Matt Haberland, Tyler Reddy, David Cournapeau, Evgeni Burovski, Pearu Peterson, Warren Weckesser, Jonathan Bright, Stéfan J. van der Walt, Matthew Brett, Joshua Wilson, K. Jarrod Millman, Nikolay Mayorov, Andrew

R. J. Nelson, Eric Jones, Robert Kern, Eric Larson, CJ Carey, İlhan Polat, Yu Feng, Eric W. Moore, Jake VanderPlas, Denis Laxalde, Josef Perktold, Robert Cimrman, Ian Henriksen, E.A. Quintero, Charles R Harris, Anne M. Archibald, Antônio H. Ribeiro, Fabian Pedregosa, Paul van Mulbregt, and SciPy 1.0 Contributors; Nature Methods, 17(3) 261-272 (2020) http://doi.org/10.1038/s41592-019-0686-2

36. [pandas-dev 2020] pandas-dev/pandas: Pandas; The pandas development team; Zenodo (2020) http://doi.org/10.5281/zenodo.3509134